RADAR INTERFEROMETRIC ANALYSIS OF MINING INDUCED SURFACE SUBSIDENCE USING PERMANENT SCATTERER

D. Walter[1], **J. Hoffmann**[2], **B. Kampes**[3], **and A. Sroka**[1]

[1]*University of Mining and Technology, Department of Mine Surveying and Geodesy, 09599 Freiberg, Germany, diana.walter@student.tu-freiberg.de, Anton.Sroka@tu-freiberg.de*
[2]*German Aerospace Center (DLR), German Remote Sensing Data Center (DFD), 82234 Wessling, Germany, joern.hoffmann@dlr.de*
[3]*German Aerospace Center (DLR), Remote Sensing Technology Institute (IMF), 82234 Wessling, Germany, bert.kampes@dlr.de*

ABSTRACT

We apply the permanent scatterer (PS) technique to interferometric ERS SAR observations to analyse the surface subsidence induced by hard coal mining activities at the "Prosper-Haniel" mine (Ruhr region, Germany). Underground mining causes extensive subsidence of serveral meters and typically high subsidence rates at the earth's surface. We show that this approach is applicable for the measurement of displacements in underground mining based on long time-series. A condition for a successful derivation of subsidence on the PS is the integration of model data in the processing of the PS system. We use about 78 ERS-1/-2 scenes for our analysis. Extensive validation data are also used to constrain the spatial and temporal displacement field and verify the interferometric results.

Key words: subsidence, hard coal mining, SAR interferometry, permanent scatterer.

1. INTRODUCTION

Underground mining usually causes extensive subsidence of serveral meters at the earth's surface. Particulary in densely populated areas these effects result in significant damages to houses and urban infrastructure. Mining companies in Germany are required by law to compensate for the damages. To prevent unjustified claims the mining companies are interested in the area-wide accurate monitoring of the surface subsidence. At the moment the coverage of subsidence information with precise levelling is very expensive and time consuming. Due to the pointwise measurement, this procedure cannot provide area-wide spatial information and the high costs inhibit the frequent updating of the data.

An alternative method for detecting and analysing subsidence is provided by radar remote sensing, namely differential radar interferometry (DInSAR). Differential radar interferometry is well suited to detect small relative displacements of the surface. This fact is mainly due to the short wavelenght of radar signals (cm). The fundamental measurement value of this method is the phase of the radar signal. An important condition for successful interferometric analysis is a high coherence between the radar signals. Unfortunately, interferometric analysis of radar data in central Europe is often hampered by extensively vegetated land surfaces that can destroy the deterministic phases differences in temporally separated images. Longer temporal separations between two radar acquisitions typically reduce the ability to interpret the measured phase differences. Another source of reduced signal coherence or decorrelation, is the geometric difference in the incidence angles between two aquisitions [11]. Furthermore high subsidence rates, which are typical for mining, can reduce the deterministic coherence of radar data [7].
The recently developed "permanent scatterer" technique [2] now enables the construction of much longer time-series of displacement measurements than previously feasible. This method identifies scatterers in the radar images that remain coherent over a long time and a wide range of viewing angles by means of statistical analysis. Displacement measurements are then exclusively made at these points.
In this study we use the DLR interferometric system extented for permanent scatterer processing technique [1, 4]. We demonstrate the possibility for appling the PS technique to derive mining induced subsidence with high subsidence rates. The analysis was carried out using 78 ERS-1/-2 scenes acquired between 1992 and 2000. The area under investigation is located in the Ruhr region of Germany over a hard coal working area (panel) of the "Prosper-Haniel" underground mine of the DSK AG. In situ hard coal seams occur in inclined bedding. In the mine the thickness of extracted hard coal seams reached 4

Proc. of the 2004 Envisat & ERS Symposium, Salzburg, Austria
6-10 September 2004 (ESA SP-572, April 2005)

meters in a middle depth of 890 meters in longwall working with a face width of 400 meters and lenghts of 1 to 2.5 kilometers. The maximum subsidence at surface in this mining area was 4 meters during 1992-2000. The active panels of about 55 km^2 are mostly located under the ”Kirchheller Heide” nature preserve. Since permanent scatterer points are primarily found on man-made objects, the permanent scatterer analysis could only be performed for one investigated active panel covering several small towns. A key element of the presented study is the integration of model data into the permanent scatterer system. This was necessary for the accurate derivation of the high subsidence rates occuring in the context of mining. The first part of this paper provides an overview of the fundamentals of mining surface subsidence and the possibility of a calculation of expected subsidence. Thereafter we present the integration of this calculation into the DLR permanent scatterer system in the interferometric data processing. In the last sections the expected and obtained results of the subsidence estimation in mining using PS technique are presented and discussed.
More details on the study presented in this paper is found in [9].

2. MINING INDUCED SUBSIDENCE

The underground mining of mineral deposits from the rock mass system of the earth creates large underground excavations. In mining without back-filling (clastic rock, sand, ash etc.), the openings are closed sooner or later because of the overburden pressure of the top and side rock mass layers. As a result, the subsidence of the roof above the opening has an effect on the earth‘s surface. The deeper the opening the shallower and wider the subsidence basin is, depending on the structure of rock mass [5].
Typical of the german deep-level hard coal mining is the formation of an extensive and shallow subsidence trough. The shape of this depends on mining depth, the worked seam thickness and the extent of the mining, as well as on tectonic faults and the method of mining, the speed of advance, the back-filling and the rate of stress to strata due to multiple-seam mining. The basic theory of the ground movement due to mining operations was advanced by Lehmann‘s trough theory in 1919 [6]. The maximum vertical subsidence is reached in the centre of the affected area. The amount of maximum subsidence depends on the mining depth and extent. For mining of the so-called ”critical area of extraction” the maximum subsidence Δz_{Max} can be computed from the working thickness *m* and an empirical subsidence factor *a*. The subsidence factor *a* is an empirical value for the loosening of overlying rock depending on filling and is 0.9 for mining with self-filling (without back-filling) for example [5]. For any point *i* on the surface the maximum subsidence Δz_{Max} will be reduced by a ”factor of effect” *e(i)* (see eq. 1).

$$\Delta z(i) = e(i) \cdot \Delta z_{Max} = e(i) \cdot a \cdot m \qquad (1)$$

There is a delay of the subsidence at the surface with respect to the advancing coal face (see fig. 1) [5]. Curve 1 shows the temporal subsidence at point P at the earth surface above the excavation. The temporally increasing effect of mining on point P relative to the maximum subsidence at this point can be seen in curve 2. The difference of these two curves is the time delay curve. For mining induced subsidence the rate of subsidence typically increases initially, while the mining approaches point P, and decreases during the departing phase of the moving coal head (face). This results in a highly non-linear subsidence history.

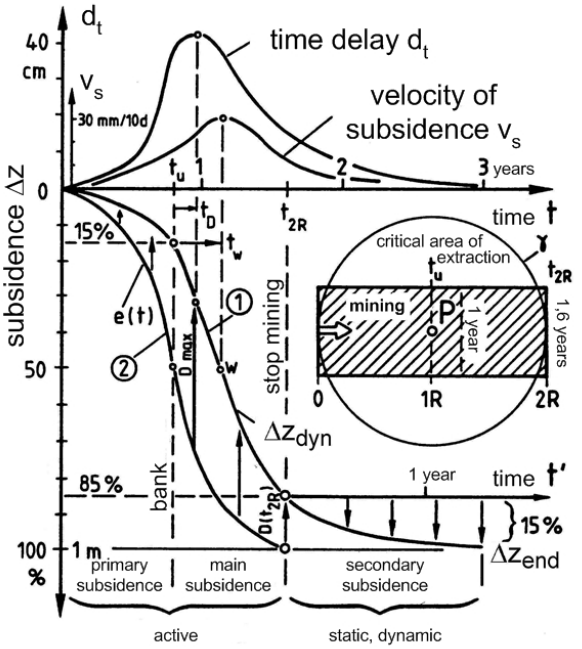

Fig. 1. The subsidence history of a point P in relation to the moving coal head (curve 1) and the temporal effect of mining in terms of the maximum subsidence at the point P (curve 2). The other curves show the velocity and time delay of subsidence. [5].

2.1. Calculation of expected subsidence

The calculation of expected subsidence is very important for the estimation of potential mining damages and particularly to determine the extent of subsidence. Furthermore it is interesting with respect to preventing structure damages prior to mining and reparation afterwards [5]. For the calculation mathematical models are necessary. These should be described by the correlation between the compression of excavation and the ground movement (cause $\Leftrightarrow$ effect). The difficulty is the insufficient knowledge about the mechanical properties of the rock mass deforming due to mining activities. There are many methods for calculating expected subsidence [5].

The DSK AG predicts the ground movements (vertical and horizontal displacement, tilt, tension and compression etc.) using the AutoCAD application *CadBERG* [10]. This system is based on a stochastic method considering mining parameters, including the geometry of the excavation and the temporal development (see section 2). The effect of an elementary excavation on a point at the surface can be described using a transfer function, in this case a Gaussian distribution. The mining block is rasterized and a mining depth, the limit angles of the subsidence effect and other mining parameters are assigned to each raster element. The dynamics of temporal subsidence is included using an e-function $q(t)$ developed by *Knothe* in 1953:

$$q(t) = 1 - e^{-c\cdot(t-t_0)} \qquad (2)$$

The exponential time coefficient c characterizes the propagation behavior of the rock mass system in the opening process. The dynamic subsidence of a surface point at a particular time results from the product of eq. 1 and eq. 2. The total effect of the mining at the surface is the result of the sum of the effects of all raster elements.

3. DATA PROCESSING

The measurement of mining induced subsidence was conducted using the DLR permanent scatterer system [1, 4]. The available ERS scenes, acquired nearly every 35 days, were a very good basis for this interferometric analysis. These radar scenes have perpendicular baselines from 7 meters to 1037 meters. The steps for the calculation of diffential interferograms were similar to those in classical DInSAR processing. All scenes were coregistered geometrically to a selected *master* scene using an external DEM (SRTM-ERS mosaic, accuracy: 2-22m). Subsequently we computed 77 interferograms. The average coherence of most interferograms was very low with a maximum of 0.31. Vegetation and high rate of subsidence caused severe decorrelations (fig. 2). The interferograms were corrected for topography using the external DEM. Because of the insignificant topography in the region of Prosper-Haniel (20-70m), most visible fringes in the interferograms can be interpreted as movements of the surface (fig. 2). The fringes indicated by arrow 1 in the lower frame of fig. 2 are caused by subsidence within the area of influence of the Prosper-Haniel mine.

The permanent scatterers were detected by an analysis of the temporal backscattering behavior of point scatterers in calibrated images. The aim of this processing step was to find as many scatterers as possible because a subsidence pattern has to be sampled spatially as densely as possible [1]. Because of the low density of PS in the nature preserve above the working area of the Prosper-Haniel mine (see fig. 3), we chose a larger area of estimation to construct a connecting network on both sides of that region to enable a meaningful spatial interpolation of subsidence values. The objects, which were identified as permanent scatterer in this area were often industrial buildings, greenhouses and other man-made features with point-like backscattering characteristics.

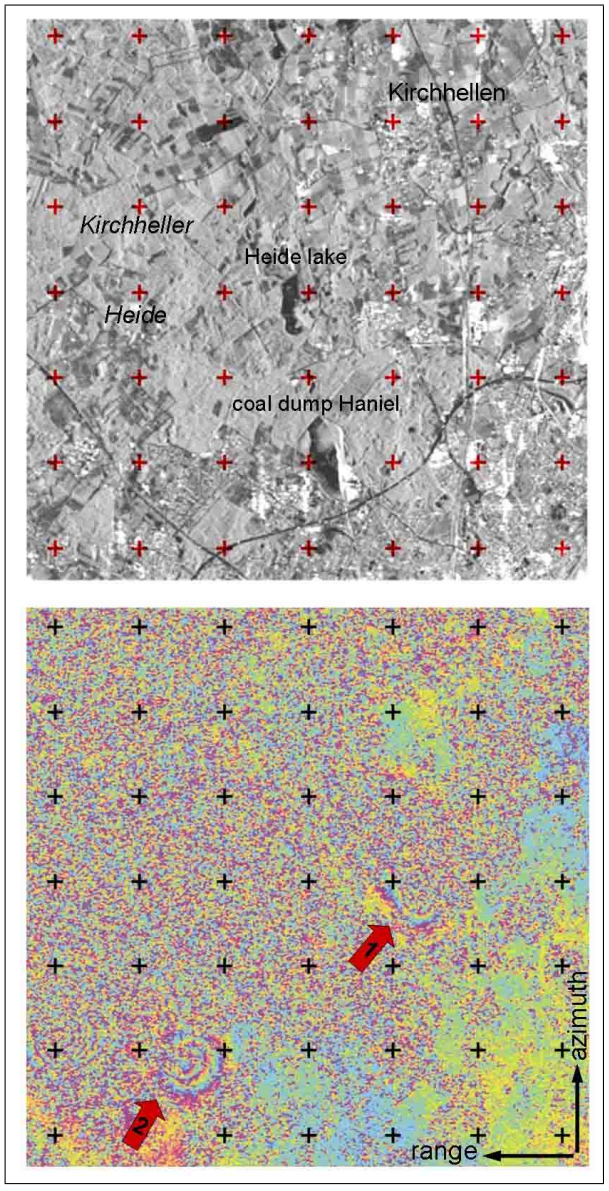

Fig. 2. The mean radar amplitude of all ERS scenes (above) and the interferogram with a perpendicular baseline of 70 m and a temporal baseline of 175 days (below). The visible fringes were caused by mining induced subsidence of the Prosper-Haniel mine (arrow 1) and a neighboring hard coal mine (arrow 2).

In general, the next step of PS processing would have been the estimation of the parameters at the PS, i.e. the subsidence rate. But because of the very high rate of subsidence in mining a robust estimation of the parameters was impossible. To circumvent this problem, we integrated from the CadBERG predictions asdescribed below. The next step of PS processing was the temporal

phase unwrapping [3], i.e. the estimation of differences of DEM errors and the displacement rates in line of sight (LOS) between PS (arcs). Furthermore a least square adjustment and statistical testing were used to obtain the measurement values of subsidence rate and DEM error at the PS. Statistical tests were applied to identify and remove unreliable points and arcs, until a stable solution for estimation was reached [4].

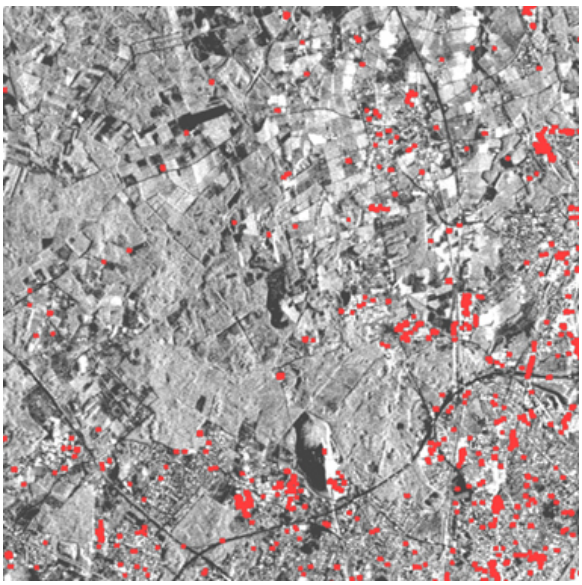

Fig. 3. Overlay of the detected permanent scatterers (red) on the intensity image of the working area of the Prosper-Haniel mine.

4. INTEGRATION OF MODEL DATA

The mining caused surface subsidence of serveral meters. For a robust measurement of subsidence using the DInSAR method, very frequent radar acquisitions would be necessary. Alternatively radar images recorded by sensors with a longer wavelenght than ERS (5.6 cm) could be used. But for the available ERS differential interferograms a cycle of phase is equivalent to a vertical displacement of about 3 cm. For the repeat cycle of ERS of 35 days we calculated (using CadBERG) an average maximum subsidence of 23 cm. The radii of the calculated subsidence bowls were typically on the order of 1000 m. Furthermore the temporal movement of the points at the surface is non-linear (see fig. 1), whereas the DLR PS system assumes a primarily linear motion. In a recently developed version an arbitrary base function can be chosen, but it proved very difficult to find a sufficiently general function for the description of mining induced subsidence (fig. 4).
In this study we used the advantage of stochastical models such as the calculation of expected subsidence with CadBERG. As a recalculation the computations take into account the actual mining and mining geometry.

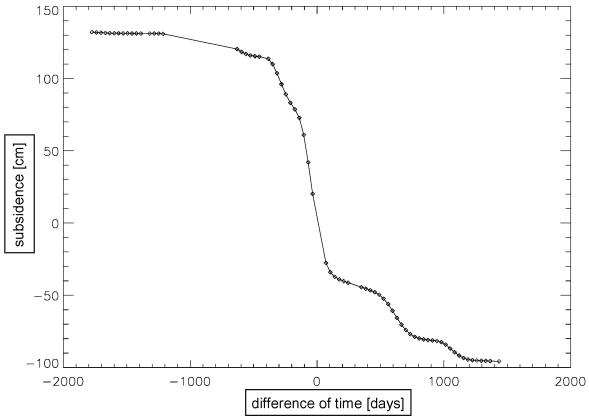

Fig. 4. The calculation of expected subsidence of a point, near the centre of maximum subsidence caused by the multiply-seam mining of Prosper-Haniel between 1992 and 2001.

This model data was calculated dynamically between two successive radar acquisitions with a theoretical time stage function for points of a regular grid (25m x 25m) in the German Gauss-Krueger projection. The modeled subsidence were referenced to the time of the master scene. In this way it was possible to simulate theoretical radar interferograms with the assumption that coherence equals 1 and the differential phase equals the phase of movement (deformation). This was realized by common equations of radar interferometry and ERS parameters, see eq. 3 with eq. 4. Horizontal displacements were not considered. As a basic principle there maximum is located above the mine working boundary of highest subsidence and is approximatly 20%-40% of the maximum subsidence, i.e. decimeter [8].

$$\phi_{DInSAR} = \frac{4\pi}{\lambda} \cdot \Delta r_{Diff} \tag{3}$$

$$\Delta r_{Diff} = \Delta z \cdot \cos\theta \tag{4}$$

With λ - wavelength, Δr_{Diff} - displacement in LOS, θ - look angle and Δz - vertical displacement (subsidence).

The wrapped phase was computed from the unwrapped phase. The comparison between the simulated theoretical interferogram and the result of InSAR processing in fig. 5 shows a good agreement in terms of the fringe pattern. Above, in the right side of fig. 5 strong decorrelation in the centre of the basin of subsidence occurs even in the 35day interferogram. This is due to the high subsidence gradient. The poor coherence to the left of this area is due to the existence of vegetation. The higher the temporal baselines between master and slave scene, the stronger is the decorrelation of the differential interferograms.

In integrating the model data the accurate geocoding was very important. We transformed the radar coordinates of the PS to the projection of model data, i.e. Gauss-Krueger coordinates. After this we interpolated the simulated subsidence (available in a raster of 25 m $\times$ 25 m) at the geocoded PS positions. Finally, the model data at PS positions were converted to phases according to eqs. 3 and 4 and subtracted from the differential interferometric phases of PS.

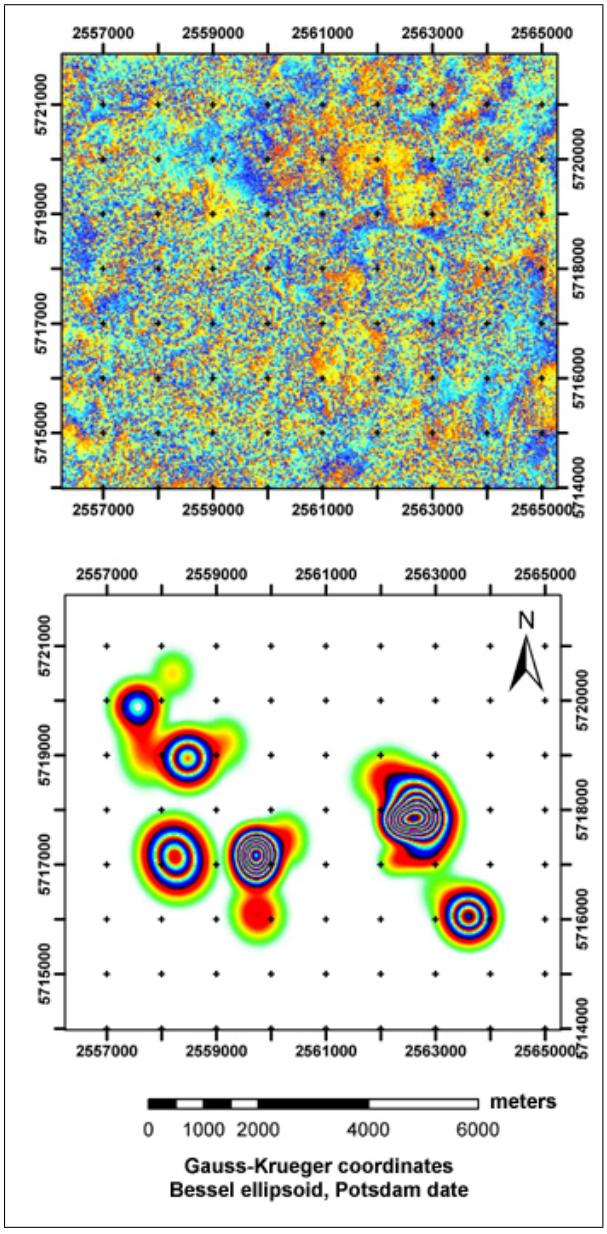

Fig. 5. Comparision of geocoded interferogram (35days) (above) and the simulated theoretical differential interferogram (below) for total effected area the Prosper-Haniel mine.

In the result we used model corrected differential phases to estimate deviations between model data and precise levelling on benchmarks (reality) using DLR permanent scatterer system. This means that we estimated the residues of subsidence, because the high-subsidence (model) were already substraced from differential phases.

5. ANALYSIS METHOD AND EXPECTED RESULTS

The subsidence estimates were analysed and assessed by comparing them to the results of precise levelling surveys. Since we estimated only the model deviations (because of previous model integration), we compared our results with expected model deviations. The basis was precise levelling data on benchmarks, which were bilinearly interpolated at the PS positions. Precise levelling was conducted every two years (1992, 1994, 1996, 1998, 2000) by the mining companies. For the comparison with the PS estimation and computed model data, the precise levelling data at PS also had to be temporally interpolated from the nearest satellite acquisition times. Here we used a simple linear interpolation. The difference between model and levelling data at PS for 4 satellite acquisition times referenced to 1992 was equal to expected model deviations. The expected model deviations showed that the linear subsidence model was generally valid. As mentioned before, mining induced subsidence are non-linear. This non-linearity was largely eliminated for most points of the estimation by the model integration. The higher model deviations migth be due to the effects of multiple-seam mining resulting in a higher velocity of subsidence in the investigated panel of the Prosper-Haniel mine. This was not reflected in the input parameters in the calculation by CadBERG. Consequently, the calculation of expected subsidence in this mining panel was too conservative.

6. RESULTS AND DISCUSSION

We estimated a maximum linear subsidence rate (model deviation) of 78 mm/year at the PS with the maximum expected subsidence rate. A good spatial agreement between the estimated and expected results at the PS was observed (fig. 6). This indicates a successful PS estimation. However fig. 6 also shows an underestimation of the expected model deviations of up to 21 mm/year in the area of investigation. The estimated DEM error at the PS was less than 20 meters, which is within the accuracy of the DEM. Only at very few PS the DEM error was unrealistically large.

In addition to the linear estimation of model deviation we analysed the non-linear component of movement. This could be derived from the residual phases at the PS, which were the differences between linearly estimated phases and the differential phases of DInSAR modulo 2π. The residual phases are composed of atmospheric, noise and non-linear motion phase components. The aim of this analysis was the separation of these components using suitable filters. After a phase unwrapping of the

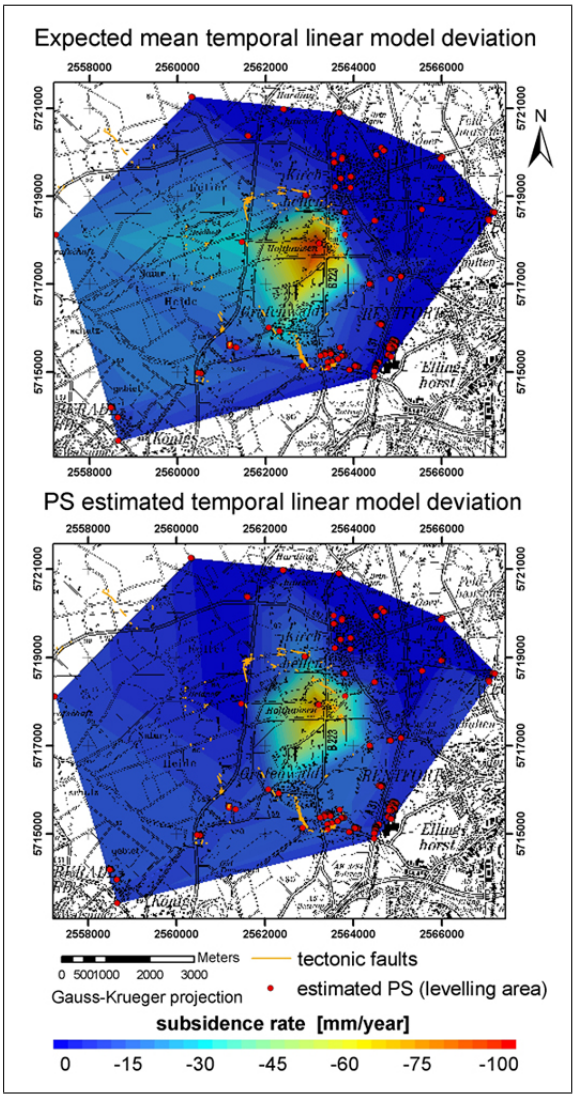

Fig. 6. The comparison between the expected mean (above) and estimated (below) temporal linear model deviations for the reliable estimated PS in the area of the Prosper-Haniel mine

residues, we filtered the total signal, i.e. the sum of absolute phase of model data, estimated linear model deviation and residues. A small temporal shift of the modeled phases can introduce a high-frequency signal in the total phase. This high-frequence signal can not be differentiated from atmospheric phase contributions. We eliminated the noise using a small triangle high-pass filter in space, because the atmosphere and the non-linear movements are correlated either in space. With a small triangle low-pass filter in time (35days) we tried to divide atmosphere and noise from the non-linear phase component. A higher filter size would result in the blurring of the times of mining initiations.

The overall result of the PS estimation is shown by means of diagrams of subsidence for a few reliable estimated PS over the investigation panel of the Prosper-Haniel mine, see PS overview in fig. 7. The results of the PS estimation were added to the substracted model data at the beginning. As one can see in fig. 8, we could reached a good accordance between precise levelling and the estimation on this PS. The maximum subsidence difference between model data and the real measurement (precise levelling) was 12 cm during 1992 and 2000. After the estimation, the maximum difference was only 4 cm. The high frequencies of the curve of estimated subsidence were the result of the weak filter for non-linear motions in time. The right side of fig. 8 show a good accordance between the expected result and the PS estimation of model deviation. The greater differences in last times (1998, 2000) could be due to errors in the phase unwrapping of the residues.

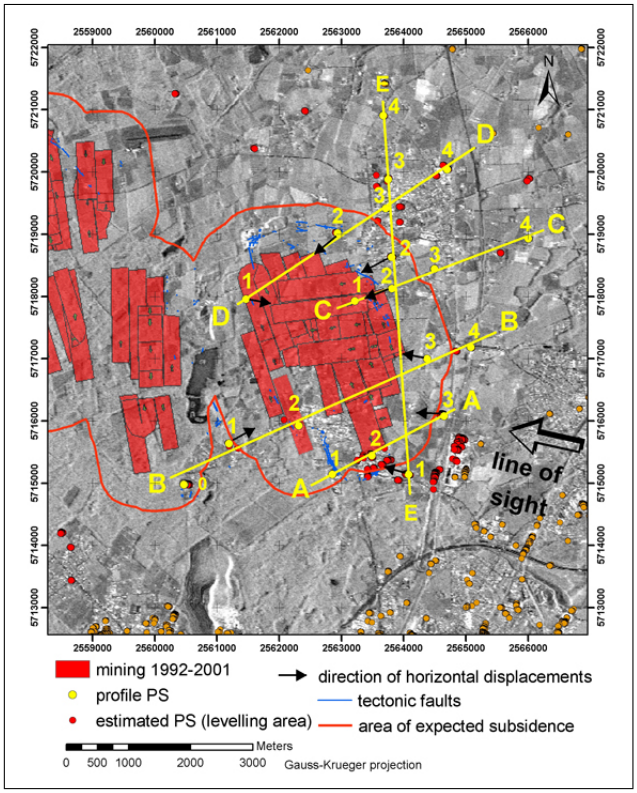

Fig. 7. The overview of the mining during 1992-2001 and the estimated PS in the area of Prosper-Haniel. The analysis of PS estimation was taken along the profiles for the sparse detected PS.

Even if the calculated subsidence was small for a PS, finally we got a good result for PS estimation (see fig. 9a). In comparison to the calculated model data of the Prosper-Haniel mine the PS estimation was more precise. A relatively good acquisition of the subsidence was obtained in the southern area of the investigated mine panel of Prosper-Haniel (fig. 7, profile A) and in the border zone of influence of mining. Problems appeared in the context of PS with high model deviations. One reason for PS estimation errors was an erroneous temporal phase unwrapping, which could be detected by observations at the estimated arcs. The different model deviations of two points connected by an arc was the reason for this, because the parameters are first estimated for the arcs and

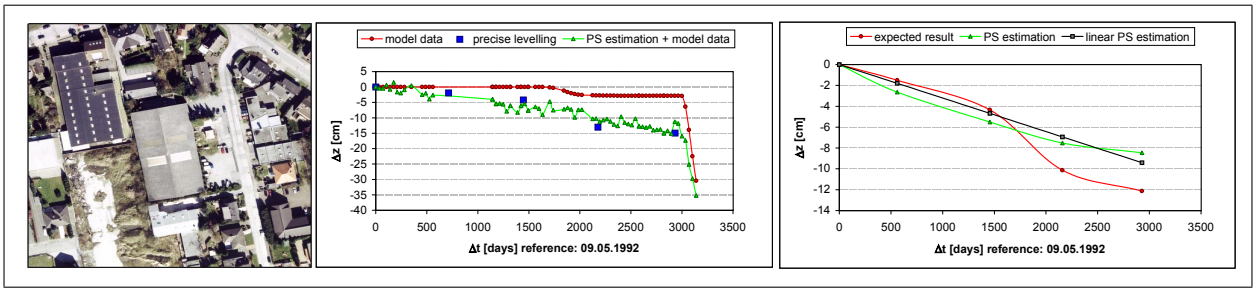

Fig. 8. Analysis of PS estimation of the profile point A2. The aerial view on the left side shows the object, which was detected as PS, mainly due to its the favorable geometry and backscatterer behavior. The first diagram (center) shows the comparison between the model data, the precise levelling and the PS estimation including the model data. On the right side, the expected and estimated model deviations are compared.

then integrated to the points. Such differences often appeared on tectonic faults (fig. 7), that were not considered in the calculation of the expected subsidence. An example for such a phase unwrapping error is illustrated in fig. 9b. Another source of error for the appropriate derivation of subsidence from the PS was a wrong spatial phase unwrapping of the residues and the incomplete separation between atmospheric, noise and non-linear components of the residues. For example in fig. 9c, the high noise prevents the successful derivation of subsidence. Nevertheless the trend of estimation corresponded with the precise levelling data. Biases result from horizontal displacements of PS, which were not considered in the model data integration. An example of this is shown in fig. 9d. The underestimation for this PS as of 1996 (Δt=1446 days) suggests the presence of horizontal displacements because the point D1 has moved toward the ERS sensor against line of sight (fig. 7). Fig. 7 illustrates the assumed horizontal directions of few PS. Given the radar aquisition geometry the vertical underestimation of 9 cm for 2000 at the point D1 corresponds to a minimum horizontal movement of 21 cm. This is realistic for a mining induced subsidence of 92 cm during 1992-2000. The profile B in fig. 10 clarifies the effect of horizontal displacements on PS estimation. Because of the increase in horizontal movements in direction of the working boundary of mining there was an increasing of underestimation of the real subsidence using the PS system (see fig. 7). The opposite effect is shown of point B3. There is no consideration of data from 1993, because of inaccurate temporal interpolation from precise levelling for this year.

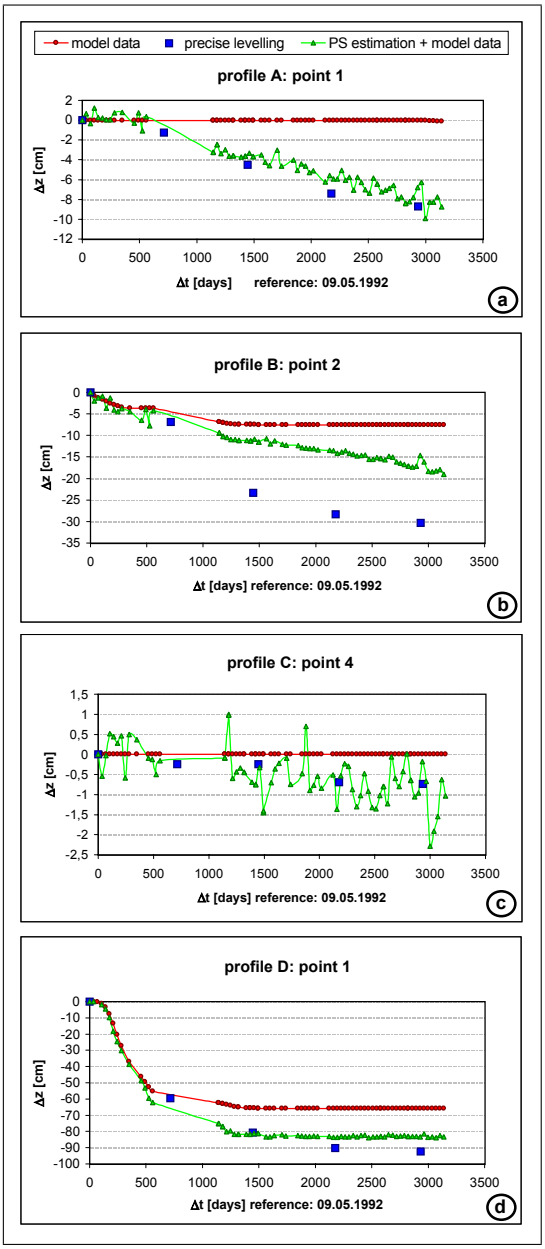

Fig. 9. Other examples for comparison of subsidence on the estimated PS along the profiles of fig. 7

7. CONCLUSIONS

The most important limiting factors for the derivation of mining induced subsidence using the PS technique are the typically high rate of subsidence and the low density of detected permanent scatterers. Nevertheless, this study has shown that the estimation of this subsidence using PS technique can be feasible by integrating model data. Depending on the density of PS there was a good spatial differentiation of area influenced by mining or rather the area of model deviations. The PS estimation was not

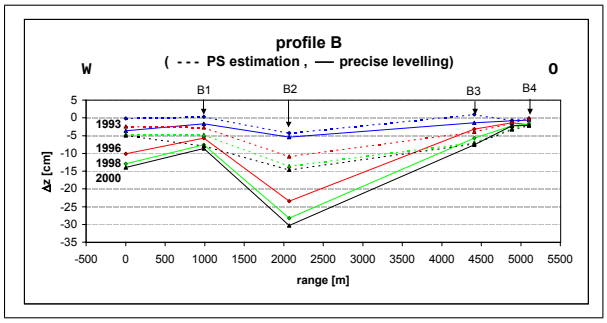

Fig. 10. Comparison between the subsidence derived from precise levelling and the PS estimation inclusing the model data along the profile B in reference to 1992.

possible in some areas with vegetation, e.g. in the Kirchheller Heide, because of a lack of detected PS. Despire the poor coherence of the differential interferograms and few visible fringes we could estimate the subsidence on PS for a large time span of 8.5 years. We improved the agreement between the subsidence measured by precise levelling and the model-estimated results. A quantitative specification of accuracy in terms of the derivation of mining induced subsidence using PS technique is not possible, because of the complexity of the errors. But here we have tried to show the limitations of the PS method in mining applications by discussing the errors. Under ideal conditions, i.e. a high density of detected PS and the integration of model data with higher accuracy, should be able to detect mining induced subsidence with an accuracy of millimeters or centimeters. A prerequisite for this is the successful separation of the residual phase components.

Future research should integrate calculations of expected horizontal displacements. Furthermore to increase the accuracy of the model data, the parameters of the calculation of expected subsidence should reflect for example the frequency of extraction in the mining.

The application of the PS method in mining regions with most favorable conditions for the interferometric analysis of subsidence, for example with less vegetation, would lead to better results. Mainly we expect a better utilisation of PS technique in urban areas with underground mining for example in other underground hard coal mines of the Ruhr region in Germany, because of the detection of more PS. In the future it is imaginable to use radar interferometric analysis with PS technique in combination with the current monitoring for the observation of mining induced subsidence. A higher temporal and spatial resolution can be achieved for observations with a higher density of permanent scatterers. The integration of the model calculation in the PS system can also be a interesting topic for future studies. This might enable new insights into rock behaviour or the location of faults.

REFERENCES

[1] N. Adam, B. Kampes, Eineder M., J. Worawattanamateekul, and M. Kircher. The development of scientific permanent scatterer system. In *Proc. ISPRS Joint Workshop on "High Resolution Mapping from Space" 2003*, Hannover, Germany, 6-8 October, 2003.

[2] A. Ferretti, C. Prati, and F. Rocca. Permanent scatterers in SAR interferometry. *IEEE Transaction on Geoscience and Remote Sensing*, 39(1):8–20, 2001.

[3] R. F. Hanssen. *Radar Interferometry - Data interpretation and error analysis*. Kluwer Academic Publishers, Dordrecht, Netherlands, 2001.

[4] B. Kampes and N. Adam. Velocity field retrieval from long term coherent points in radar interferometric stacks. In *Proc. IGARSS 2003*, Toulouse, France, 21-25 July, 2003.

[5] H. Kratzsch. *Bergschadenkunde*. Deutscher Markscheider-Verein e.V., Bochum, Germany, 1997.

[6] K. Lehmann. Bewegungsvorgaenge bei der Bildung von Pingen und Troegen. *Glueckauf*, 20, 1919.

[7] V. Spreckels, U. Wegmueller, T. Strozzi, J. Musiedlak, and H.-C. Wichlacz. Detection and observation of underground coal mining-induced surface deformation with differential SAR interferometry. In *Proc. ISPRS Joint Workshop on "High Resolution Mapping from Space" 2001*, Hannover, Germany, 19-21 September, pages 227–234, 2001.

[8] A. Streerath. Analyse und Modellierung grossraeumiger bergbaubedingter Senkungen aus photogrammetrischen Beobachtungen. Ph.D. thesis, TU Clausthal, Germany, 2000.

[9] D. Walter. Untersuchung der vom untertaegigen Bergbau induzierten Senkungen unter Verwendung der Permanent Scatterer Technik als Methode der differentiellen SAR Interferometrie. diploma thesis, Department of Mine Surveying and Geodesy, University of Mining and Technology, Freiberg, Germany, 2004.

[10] R. Wieland. CadBERG - Eine kurze Einfuehrung ueber das Verfahren zur Vorausberechnung von Gebirgs- und Bodenbewegungen, 2001. User manual: CadBERG.

[11] H. A. Zebker and J. Villasenor. Decorrelation in interferometric radar echoes. *IEEE Transaction on Geoscience and Remote Sensing*, 30(5):950–959, 1992.